Estimates of human cochlear tuning derived from DPOAE reflection-component delays

Abdala, Carolina; Guérit, François; Luo, Ping; Shera, Christopher A.

Publication date:
2013

Document Version
Publisher's PDF, also known as Version of record

ESTIMATES OF HUMAN COCHLEAR TUNING DERIVED FROM DPOAE REFLECTION-COMPONENT DELAYS

Carolina Abdala[1,2], François Guérit[3], Ping Luo[1] and Christopher A. Shera[4,5]

[1]House Research Institute; [2]University of Southern California, Los Angeles, CA

[3]Technical University of Denmark, Lyngby, Denmark; [4]Eaton-Peabody Laboratories, [5]Harvard Medical School, Boston, MA

INTRODUCTION

Cochlear delay and cochlear tuning are linked through filter theory, which holds that sharper tuning requires longer delays. Likewise, cochlear delays have been linked to reflection source OAE delays via the theory of coherent reflection (Zweig and Shera, 1995). [Reflection-source emissions denote those OAEs arising from backscattering of energy off of micromechanical irregularities along the cochlea, i.e., stimulus-frequency and click-evoked OAEs, and the reflection component of the DPOAE.] A relationship between OAE delays and cochlear tuning has been demonstrated in several species (Shera et al., 2002; Oxenham and Shera, 2003; Shera et al., 2010). However, tuning estimates derived from OAE delays measured in humans are sharper than tuning recorded in other mammals, leading to some skepticism about the proposed relationships (Siegel et al., 2005; Ruggero and Temchin, 2005, 2007).

Here we apply delays derived from the reflection component of the $2f_1$-f_2 DPOAE to estimate tuning in humans using a species-invariant tuning ratio which defines the covariation of cochlear tuning and emission delays (Shera et al., 2010). Our objective was to explore non-invasive methods for obtaining estimates of cochlear tuning and to generate preliminary tuning estimates for age groups representing seven decades of the human lifespan.

METHODS

Subjects - 186 subjects: 15 premature (mean = 34 wks PCA) and 30 term newborns; 19 six-month-old infants, 26 teens (13-16 yrs), 43 young adults (18-30 yrs), 21 middle-aged (40 - 57 yrs) and 32 older adults (68-75 yrs).

DPOAE ($2f_1$-f_2) - f_1, f_2 swept logarithmically at 8 s/oct for DPOAEs from 0.5 – 4 kHz, and 24 s/oct for DPOAEs from 4 – 8 kHz; 65 (L_1) – 55 (L_2) dB SPL; f_2/f_1 = 1.22. Least-squares fit method used to estimate DPOAE level and phase from averages of 6 to 8 sweeps.

Inverse FFT - MATLAB-based software was used to separate DPOAE distortion- and reflection-source components based on their respective phase-gradient delays. (DPOAE and IFFT software developed by C. Talmadge, adapted by P. Luo; See Abdala and Dhar, 2012.)

Loess - Simple models of linear and nonlinear least squares regression are fitted to localized subsets of the data and adjacent fits are joined to create the overall fit. Loess fits were conducted using two strategies: energy weighting and peak picking (Shera and Bergevin, 2012).

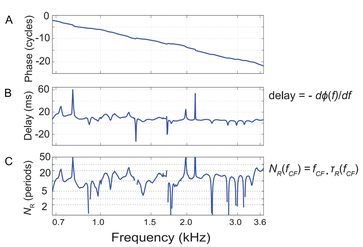

Fig. 1. Reflection-component data from one young-adult subject. (A) phase versus frequency; (B) phase-gradient delay and (C) N_R - delay in periods.

I. Calculating Delays

Fig. 2 Term Newborn

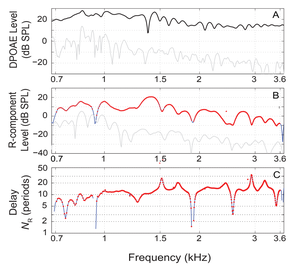

Fig. 3 Young Adult

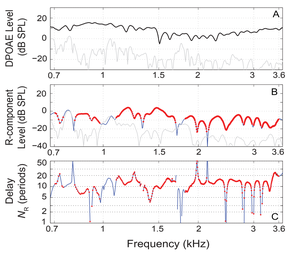

Fig. 4 Older Adult

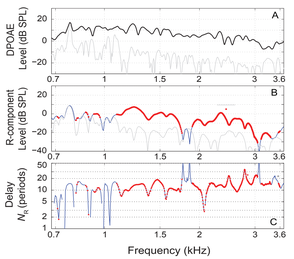

Figs. 2-4. Calculating delay in three subjects.

Panel A - DPOAE level (black) and noise (gray).

Panel B - IFFT-separated reflection or "R-component" level (blue) and reflection-specific noise floor (gray). To be accepted, data points were at least 6 dB above both DPOAE and R-component noise floor. The red points are accepted values; segments where the blue line is visible did not meet this SNR criteria.

Panel C - R-component delay normalized in periods as N_R. Only data points shown in red were used in estimating the delay trend.

Energy Weighting

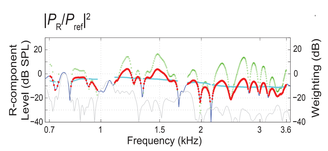

Fig. 5. Data from the young-adult subject shown in Fig. 3. Delay values are weighted by R-component energy, applying $|P_R/P_{ref}|^2$. The blue line and red points denote reflection level, P_R. P_{ref} in cyan is a local estimate of mean R-component level. The green points (re: right axis) display the weighting assigned each delay value.

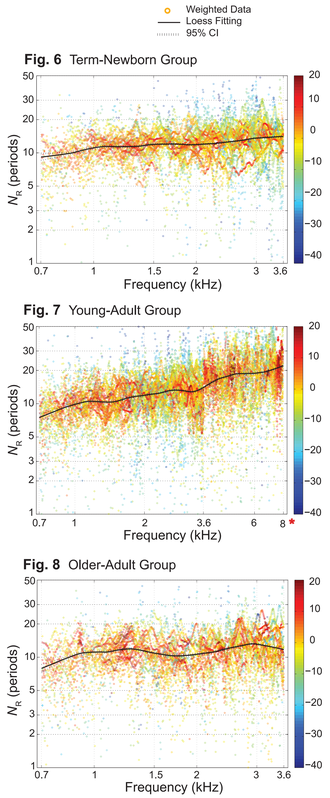

Fig. 6 Term-Newborn Group

Fig. 7 Young-Adult Group

Fig. 8 Older-Adult Group

Figs. 6-8. Energy-weighted loess fit (black line) and individual delay values (colored points) for three age groups. Weighting is denoted by color (re: right axis). NOTE: Because weighting was calculated locally, it cannot be precisely equated across frequency.

*The young-adult data are shown over an extended frequency range through 8 kHz.

II. Modeling Delay Trend

Peak Picking

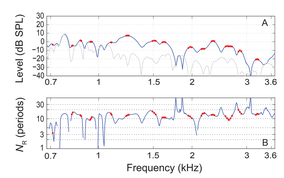

Fig. 9. R-component delay data from one young adult calculated at peaks in fine structure only. (A) A peak-picking algorithm was applied to mildly smoothed R-component level (blue line) and peaks were defined by three frequencies (red points); (B) Peak frequencies represented on corresponding delay data.

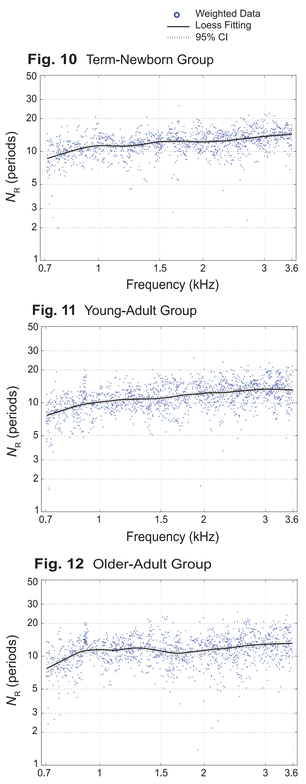

Fig. 10 Term-Newborn Group

Fig. 11 Young-Adult Group

Fig. 12 Older-Adult Group

Figs. 10-12. Loess trend line fit to R-component delay data in three age groups. Delays were taken at peaks in fine structure only.

Final Parameters: Two-pass "cleaning" with 6 dB SNR; P_{ref} window = 1 octave; loess window = 0.6 octave; final loess fit is the mean of energy-weighting and peak-picking fits.

Parameters

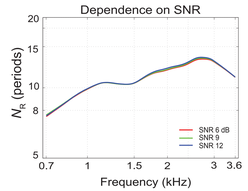

Fig. 13. Energy-weighted loess lines from the young-adult group, fit to delay data using three different SNR criteria. Increasing criterion SNR did not impact fit.

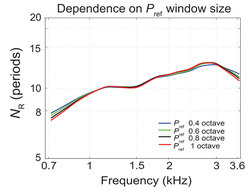

Fig. 14. P_{ref} (estimate of local R-component level for weighting) calculated with four windows in the young-adult group. Local versus more global window size did not alter the fit greatly though smaller windows produced smoother trend lines.

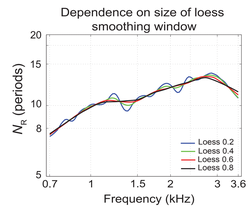

Fig. 15. Loess fit calculated using four window sizes in the young-adult group. Changing the loess window from local (0.2 octave) to more global (0.8 octave) had a strong effect on the trend line and its smoothness.

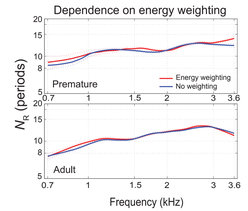

Fig. 16. With ideal (i.e., adult) data and good SNR, a weighted fit may not have a strong impact; however, with noisier data from a premature newborn, the difference is more apparent.

III. Estimating Tuning

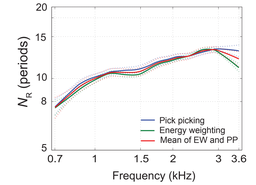

Fig. 17. The loess fit from energy weighting (EW) versus peak picking (PP) differed slightly, especially at high frequencies. A loess fit was calculated as the mean of trend lines derived from the two strategies and is shown here for the young-adult group. 95% CIs ( ) were calculated as sqrt(CI_{EW}^2 + CI_{PP}^2). The mean trend line was used in estimates of tuning.

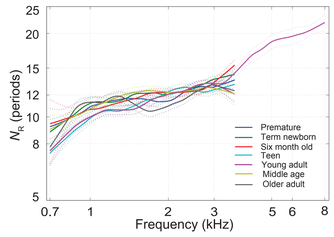

Fig. 18. Mean loess trend lines for seven age groups. There is a general increase in delay with increasing frequency and a downward bend in delay at ~1 kHz for all age groups; this bend denotes a putative apical-basal (a|b) transition and a break in cochlear scaling.

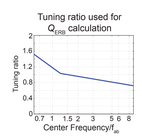

Fig. 19 (left). The tuning ratio, *r*, depicts the covariation between cochlear tuning and emission delay [$r_{species}$ = Q_{ERB}/N_{SFOAE}] calculated from cat, guinea pig and chinchilla. We assume *r* is species invariant and apply an approximate fit to our human OAE delays.

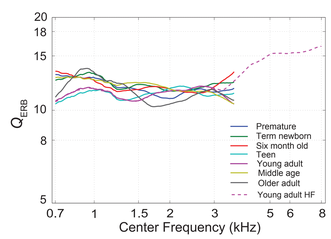

Fig. 20. To derive tuning estimates, we multiplied tuning ratio by N_R to obtain Q_{ERB}

$$Q_{ERB}(CF) = r(CF/CF_{a|b})N_R(f)|_{f=CF}$$

The a|b frequency was derived from the bend in the human delay function. The resulting Q values ranged from 9 to ~16. Infant groups showed high Q values over much of the frequency range. The adult data showed a slight decrease in tuning at the highest frequencies measured (near 3 kHz).

DISCUSSION

(1) Consistent with past work (Shera and Bergevin, 2012), these results suggest that peaks in fine structure carry the most important information for estimating delay trends.

(2) The loess fits based on energy weighting and peak picking usually agree and have generally overlapping CIs. Slight differences are restricted to the ends of the test frequency range.

(3) Consistent with theory (Shera and Guinan, 1999) and empirical observation (Kalluri and Shera, 2001), delays derived from the DPOAE reflection component are similar to SFOAE delays. Differences were likely due to methodological factors:

a) The probe strength to the reflection site at $2f_1$-f_2 is uncontrolled in the DPOAE paradigm.

b) L_1 suppresses the $2f_1$-f_2 site in the DPOAE paradigm thus impacting reflection.

(4) The bend in the DPOAE N_R delay function was centered around 1 kHz, marking the putative apical-basal transition and a deviation from approximate cochlear scaling. This bend frequency matches nicely with SFOAE delay data.

(5) Our tuning estimates are similar to SFOAE-based estimates. Shera et al. (2010) reported mean Q_{ERB} values ranging from ~11 to 19 over a comparable frequency range; these are slightly larger values than those found here (~9 to 16). Tuning generally becomes sharper with increasing frequency, most notably in the young-adult group, which had an extended frequency range.

(6) Maturation/Aging

a) Infants generally had high Q_{ERB} values, consistent with sharp DPOAE suppression tuning curves (Abdala, 1998) and steep R-component phase slopes in newborns (Abdala and Dhar, 2012).This sharpened tuning is likely due to middle-ear inefficiencies in the neonate, which reduce primary levels driving the cochlea.

b) Only adults show a decrease in tuning around 3 kHz. This may reflect degradations in tuning with age; however, it effectively disappeared once frequency was extended in young adults, suggesting an end effect of some sort.

c) The bend frequency marking the apical-basal transition (and deviations from cochlear scaling) does not vary with age; this is consistent with studies of cochlear scaling based on distortion emissions (Abdala and Dhar, 2012).

CONCLUSIONS

SFOAE delays in humans provide estimates of cochlear tuning (Shera et al., 2010). Our results suggest that the reflection component of the DPOAE can provide comparable delay data for tuning estimates. Here, loess fits to either energy-weighted delay data or data restricted to peaks in fine structure captured the underlying delay trends, and produced measures of human tuning that are similar to previous reports using reflection-source emissions.

ACKNOWLEDGEMENTS

This research was supported by the National Institutes of Health R01 DC003552 (CA), DC003687 (CAS) and the House Research Institute.